Rocket-and-wire triggered lightning in 2012 tropical storm Debby in the absence of natural lightning

J. T. Pilkey,[1] M. A. Uman,[1] J. D. Hill,[1,5] T. Ngin,[1] W. R. Gamerota,[1] D. M. Jordan,[1] W. Rison,[2] P. R. Krehbiel,[3] H. E. Edens,[6] M. I. Biggerstaff,[4] and P. Hyland[4]

Received 3 July 2013; revised 18 October 2013; accepted 18 October 2013; published 3 December 2013.

[1] Lightning Mapping Array source locations, channel base currents, and electric field waveforms are presented for a lightning flash triggered in the rainbands of 2012 tropical storm Debby. The National Lightning Detection Network reported no natural cloud-to-ground discharges within 60 km of the North Florida triggering site for at least 20 h before and 8 h after the triggered flash. Additionally, local electric field mill and wideband antenna networks show no close cloud or cloud-to-ground flashes. The triggering rocket was launched with negative charge overhead producing an electric field at the ground of 5 kV m^{-1} and in coordination with X-band, dual-polarimetric radar observations of streamers of enhanced precipitation descending from the melting level as they approached the site. The Debby flash consisted of an initial stage (IS) followed by eleven leader/return stroke sequences. The flash exhibited all the processes of normal triggered and natural cloud-to-ground lightning: leader/return stroke sequences, continuing currents, *K* events, and *M* components. Additionally, the flash exhibited several exceptional characteristics: three return stroke peak currents greater than 25 kA, one very long, 352 ms, continuing current that transferred about 35 C of charge to ground, and a relatively short, 202 ms, IS containing no initial continuous current pulses. Following a near-vertical upward positive leader attaining 2.8 km height, the IS branched and propagated horizontally at 3.5 km altitude. The flash, exhibiting strokes and continuing current, then ascended to and propagated horizontally at 5.5 km, extending about 25 km south and 15 km east. The 0°C level was near 4.5 km above sea level. It follows from the above that clouds that are not producing natural lightning can represent a triggered lightning hazard to launch vehicles and aircraft.

Citation: Pilkey, J. T., et al. (2013), Rocket-and-wire triggered lightning in 2012 tropical storm Debby in the absence of natural lightning, *J. Geophys. Res. Atmos.*, *118*, 13,158–13,174, doi:10.1002/2013JD020501.

1. Introduction

[2] Rocket-and-wire triggering of lightning at the International Center for Lightning Research and Testing (ICLRT), located on the Camp Blanding Joint Training Facility in north-central Florida, typically takes place in the presence of summertime small-scale convective storms. These storms form directly as the result of either Gulf or Atlantic sea breeze interactions with the atmosphere or from the interaction of outflow boundaries produced during the dissipating stage of those storms with the atmosphere. Given sufficient atmospheric instability for the formation of deep convective clouds with a well-developed mixed-phase region, located between the 0° and −40°C, consisting of mainly small ice particles, supercooled water, and soft hail (graupel), these air mass storms become frequent producers of lightning. Typical Florida thunderstorms have cloud-to-ground flash rates of 1.7 to 3.4 min^{-1} [*Peckham et al.*, 1984]. Nearby summer storms can produce quasistatic electric fields at ground level of 1 to 10 kV m^{-1} (physics sign convention: a positive electric field indicates the presence of negative charge overhead) [*Rakov and Uman*, 2003].

[3] In most triggered lightning experiments at the ICLRT [e.g., *Hill et al.*, 2012, 2013], a rocket trailing a grounded triggering wire is launched when both the quasistatic electric field at ground exceeds about 5 kV m^{-1} and the flash rate becomes relatively low, say, a flash every 30 s or more. In about

[1]Department of Electrical and Computer Engineering, University of Florida, Gainesville, Florida, USA.
[2]Electrical Engineering Department, New Mexico Institute of Mining and Technology, Socorro, New Mexico, USA.
[3]Physics Department, New Mexico Institute of Mining and Technology, Socorro, New Mexico, USA.
[4]School of Meteorology, University of Oklahoma, Norman, Oklahoma, USA.
[5]Stinger Ghaffarian Technologies, Kennedy Space Center, Merritt Island, Florida, USA.
[6]Langmuir Laboratory, New Mexico Institute of Mining and Technology, Socorro, New Mexico, USA.

Corresponding author: J. T. Pilkey, Department of Electrical and Computer Engineering, University of Florida, Gainesville, FL 32611, USA. (jpilkey@ufl.edu)

2169-897X/13/10.1002/2013JD020501

Figure 1. A Google Earth view of the ICLRT with the locations of the local electric field antenna network annotated. Electric field data used in this study were measured using electric field antennas E-7 and E-12 F. E-7, the southernmost antenna, is about 220 m from the field rocket launcher which is indicated by the red lightning bolt labeled LF2. E-12 F is about 180 m from the launcher.

half of such launches, an initial stage (IS), consisting of a sustained upward positive leader (UPL), typically several kilometers in length, followed by an initial continuous current (ICC), is successfully triggered. The triggering wire explodes during the ascent of the UPL, usually about 10 ms after its initiation [e.g., *Wang et al*., 1999]. There is no clear demarcation between the UPL and ICC, although generally after several tens of milliseconds, the typical time of a downward cloud-to-ground leader transit from the cloud charge to ground, the current measured at ground is classified as ICC. Often, the initial stage is followed by one or more leader/return stroke sequences, those being similar to subsequent strokes in natural lightning.

[4] Weather systems consisting of primarily stratiform precipitation, such as the inner core and some outer rainbands of tropical cylones, which exhibit little or no natural lightning activity, sometimes impact the ICLRT and produce electric fields at ground similar to those produced by air mass thunderstorms. Rocket-and-wire triggering of lightning in these conditions, which appear to be favorable from ground-based electric field measurements, have been largely unsuccessful. Such conditions existed on 24 June 2012, in the rain bands of tropical storm Debby, in which the quasistatic electric field at ground was measured to be 5 kV m^{-1}. The National Lightning Detection Network reported no cloud-to-ground discharges within 60 km of the ICLRT for 20 h before and for 8 h after the event to be discussed. Further analysis of the on-site electric field antenna and field mill networks also indicated that no lightning activity occurred during the 6 h of local operations. Aided by near real-time observations provided by a rapid scan, X-band, dual-polarimetric radar (RaXPol), at 19:16:16 UT, we triggered a lightning flash composed of an initial stage followed by eleven leader/return stroke sequences, hereafter referred to as the Debby flash. At the time of the launch, the radar indicated that the leading edge of a precipitation streamer was extending from the melting level in a stratiform rainband to the surface very near the ICLRT. *Hill et al.* [2013] noted the success of two triggering attempts associated with a descending precipitation packet (DePP) in dissipating convective cells. The leading edge of a precipitation streamer is a close analog to a DePP. A second rocket was launched approximately 15 min later, with a similar electric field at ground, but without the radar-identified precipitation streamers present. The launch was unsuccessful. Additional research is needed to determine if radar-identified DePPs and their stratiform region analogs may potentially be a useful guide for improving the success of rocket-and-wire triggering of lightning and as a hazard warning for launch vehicles and aircraft.

[5] The focus of this paper is the temporal and three-dimensional spatial VHF source locations of the initial stage and the following eleven leader/return strokes of the Debby flash as provided by a seven station lightning mapping array (LMA) [e.g., *Rison et al*., 1999; *Krehbiel et al*., 2000; *Thomas et al*., 2004; *Hill et al*., 2012]. The LMA source locations are correlated with measured channel base current and ground-based vertical electric field measurements. While, as we shall discuss, the Debby flash is unusual in several ways (e.g., low and stratiform cloud environment, relatively short-duration initial stage, a lack of ICC pulses, relatively large return stroke currents, very long interstroke continuing current, and large interstroke continuing current charge transfer), it nonetheless exhibits most of the physical processes of normal triggered and natural lightning: leader/return stroke sequences, interstroke continuing current, *K* events, and *M* components.

2. Experiment

[6] The measurements presented here in the analysis of the Debby flash represent a subset of the instrumentation network at the ICLRT, a facility at which both rocket-and-wire triggered lightning and natural lightning have been studied since 1993. The 2012 network was composed of about

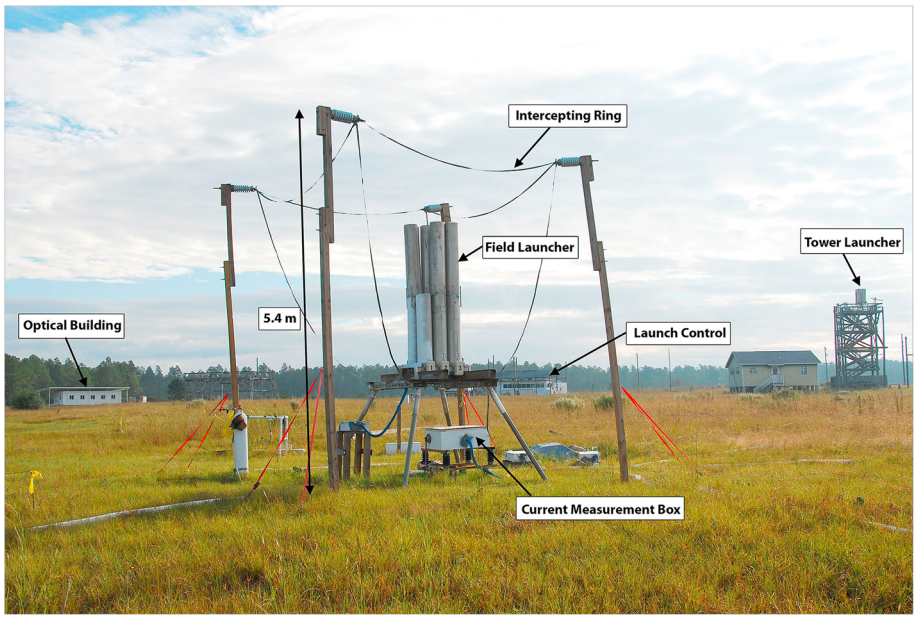

Figure 2. A photograph of the field launcher assembly from which the Debby flash was triggered. Other significant structures on the ICLRT are also identified.

90 measurements of lightning electric/magnetic fields and their derivatives, energetic radiation (X-rays and gamma rays), and optical phenomena. The measurement network spans a flat area of approximately 1 km^2. Figure 1 shows an aerial view of the ICLRT with the location of the local electric field antenna network annotated. The electric field data presented in this study were measured by electric field measurements E-7 and E-12 F. E-7 saturates at about +/−137.5 V/m with a decay time constant of 10 ms, and E12F saturates at about +/−73.2 kV/m with a decay time constant of 1.2 s. The location of the rocket launcher used to trigger the Debby flash is indicated in Figure 1 by the red lightning bolt labeled LF2. The field launcher assembly, pictured in Figure 2, consists of six rocket tubes with an overhead intercepting ring and current measurement equipment. Rocket-and-wire triggering of lightning was carried out using a 1 m long fiberglass rocket with an attached spool holding 700 m of 32 AWG Kevlar-covered copper wire. The other end of the spool was connected to the 5.4 m tall

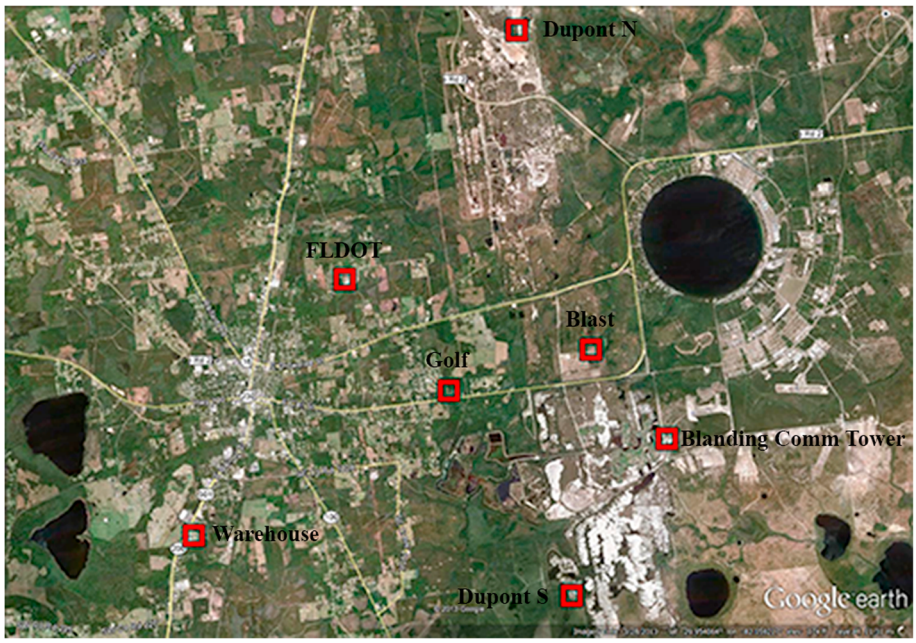

Figure 3. A Google Earth view showing the locations of the LMA stations at and around the area surrounding the ICLRT. The closest station, "Blast", is located on the ICLRT site, about 461 m northeast of the rocket launcher, LF2, indicated in Figure 1. The most distant station, "Warehouse", is located 9.6 km from the ICLRT.

Table 1. The Distance and Azimuth (Clockwise From North) Are Given for Each of the LMA Station Locations With Respect to the Rocket Launcher LF2 on the ICLRT Site (see Figures 1 and 3)

LMA Station Name:	Distance From Launcher (m):	Azimuth (Degrees):
Blast	461	64
Golf	2988	277
Dupont south	5396	188
Dupont north	7701	357
FDOT	5535	296
Warehouse	9608	252
Blanding communication tower	2773	134

grounded, metal launcher. In the event of a successful trigger, the initial stage current flows directly through the launcher with following strokes generally attaching to the overhead intercepting ring. Current was measured at the channel base with a 1 mΩ, noninductive T&M Research current-viewing-resistor in the "current measurement box" underneath and electrically connected to the rocket launcher assembly (see Figure 2). Current was measured on four different scales, spanning 1 mA to 60 kA. Additionally, observations from a number of standard HD video cameras, high speed video cameras, and still cameras complemented data collected from the measurements noted above.

[7] The spatial and temporal development of the flash was mapped by a seven station Lightning Mapping Array (LMA). The LMA is deployed at and around the ICLRT as shown in Figure 3, with one station located on the ICLRT site approximately 500 m northeast of the launcher and the next closest station about 3 km distant. Table 1 provides distance and azimuthal information of each LMA station referenced to the launcher. Each LMA station records the time of arrival and peak power of VHF sources emitted within the TV channel 4 bandwidth (66 MHz to 72 MHz), in consecutive 10 µs intervals. The VHF radiation is thought to be produced primarily by dielectric breakdown of air, usually at the tip of propagating leaders or other extending channels. A GPS receiver located at each LMA station provides a common time base for the system. LMA data are recorded locally at each station on a 120 Gb solid-state drive and later retrieved. The data are processed using a time-of-arrival (TOA) method (refer to *Thomas et al*. [2004], Appendix A) which yields temporal, three-dimensional spatial, and power information about the VHF sources as well as a reduced chi-squared value describing the goodness-of-fit of each temporal and spatial location produced from the TOA algorithm. LMA data presented in this paper are for six or seven station solutions, meaning at least six stations must have participated in the TOA algorithm, with reduced chi-squared values (a measure of goodness of fit) less than or equal to 1, assuming a 70 ns timing error.

3. Results and Analysis

[8] A 5 s time exposure of the Debby flash is shown in Figure 4. The various strokes and continuing currents are separated in the photograph by the wind which moves the lightning channel from left-to-right. This horizontal channel motion provides temporal resolution in the still photograph. The straight luminous section at the left is due to the exploded wire.

[9] LMA sources associated with the Debby flash are plotted in Figure 5. The flash is color coded based on features of the current record, beginning with the initial stage in red followed by the individual subsequent strokes grouped together, each group being displayed as one color, as follows: the no-current interval preceding the stroke, the stroke, and the continuing current following the stroke. Additionally, strokes two and three are grouped together (shown in pink color) because stroke three, with a 2.2 µs 10 to 90% current risetime, occurred in the 5.9 A continuing current of stroke two. We choose to term stroke 3 a return stroke rather than an *M* component because of its relatively fast, return-stroke-scale, risetime despite the fact that it occurs during a low level of continuing current (see Table 2). Figure 5a

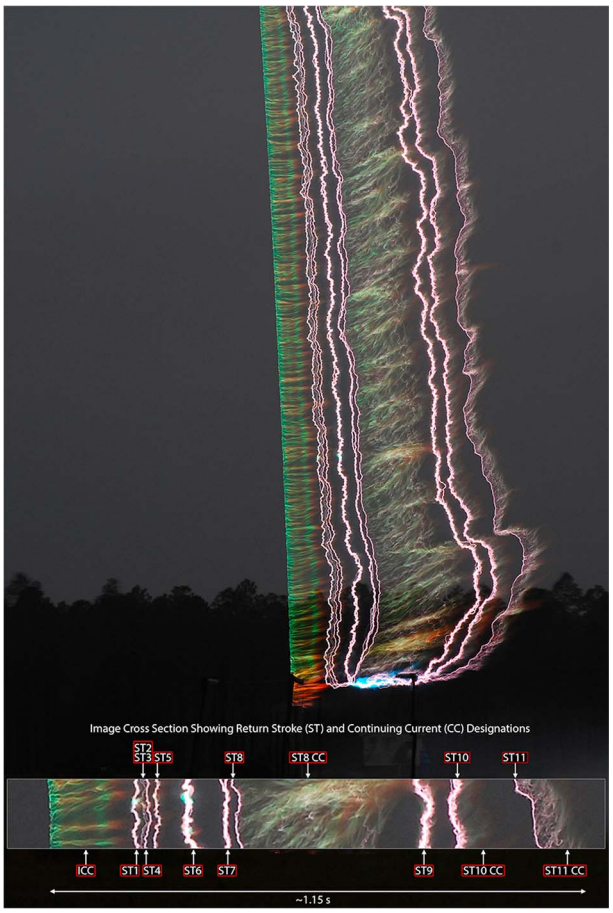

Figure 4. Five second time exposure of the Debby flash at top and an annotated section of the flash at the bottom. The wind horizontally translated the lightning channel, separating the individual strokes and continuing currents, providing temporal resolution to the still photograph. The straight luminous section at the left is due to the exploded triggering wire. The green luminosity (from the copper) following the exploded wire is produced by a steady current, referred to as the initial continuous current (ICC), flowing through the copper remnants of the triggering wire. The brightest strokes, ST6, ST7, and ST9, correspond to the strokes of highest return stroke peak currents (see Figure 7).

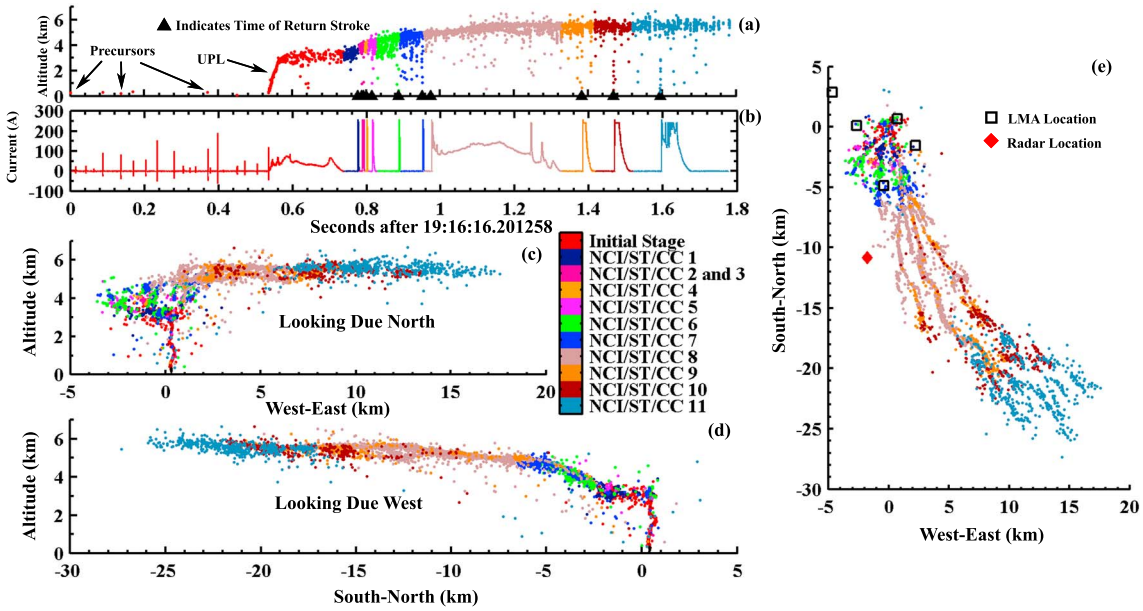

Figure 5. Four projections of LMA data. The VL channel base current is plotted and time synchronized with the LMA altitude versus time projection at the top left of the figure. The IS current duration is from 0.54 s to 0.74 s with precursor pulses, electrical breakdown at the wire tip, preceding the IS. Return strokes are marked by triangles on the time axis. The projections of the LMA data "Looking Due North" and "Looking Due West" are plotted below the current record. The plan view, or top down view, is shown on the right with the locations of five of the LMA stations and the Dual Polarization Radar annotated.

shows the altitude versus time projection of the flash with the times of the return strokes indicated by the small black triangles on the time axis. In Figure 5b, below the altitude versus time projection, the "very low (VL)" current record is time synchronized to the altitude versus time projection and color coded in the same way as the LMA sources. Projections of the flash looking due north and due west are shown in Figures 5c and 5d, respectively. Figure 5e shows the plan (top) view of the flash with the locations of five of the LMA stations annotated. In the plan view, the red diamond indicates the location of RaXPol radar. Figure 6 shows a range-height indicator (RHI) scan (a vertical scan) of the radar reflectivity in dBZ, from the RaXPOL radar at 19:16:09 UTC, about 7 min prior to the Debby flash, with the LMA sources from the flash overlaid.

[10] The Debby flash spanned a horizontal area of nearly 180 km^2, the horizontal extent of the flash reaching 25 km south and 15 km east of the initiation location at the ICLRT. Initially, the upward positive leader (UPL) propagated to an altitude of 2.8 km, deviating little from the vertical, followed by extensive horizontal branching with LMA sources located between 2.4 and 3.6 km in altitude. Following the initial stage and the first four return strokes, the flash ascended and propagated above the 0 °C level, which was at approximately 4.5 km (determined from Jacksonville sounding taken at 12 UT). The LMA sources associated with the first four strokes were located between 2.8 and 4.4 km altitude, at or below the 0 °C level. Most of the horizontal propagation occurred around 5.5 km altitude, during the continuing current following the eighth stroke.

[11] The analysis of the Debby flash that follows is subdivided into two sections. (a) Analysis of statistical parameters of the initial stage and the following strokes related to the current record and comparison to previous, similar results of such analyses of more typical rocket-triggered lightning [*Fisher et al.*, 1993; *Wang et al.*, 1999; *Miki et al.*, 2005; *Hill et al.*, 2012]. A brief comparison to similar parameters of natural lightning, observed on instrumented towers in Switzerland by *Berger et al.* [1975], will also be given. (b) Analysis of LMA data with correlated electric field and current records for *K* changes, dart leaders, continuing currents, and *M* components.

3.1. Statistical Analysis

3.1.1. Overview

[12] The channel base current waveforms from two different sensitivity scales used in the following statistical analysis are plotted in Figure 7 using the same color code as Figure 5. The peak currents, 10 to 90% current risetimes,

Table 2. The Peak Current, 10 to 90% Current Risetime and Continuing Current Duration Above About 2 A Are Given for Each of the 11 Return Strokes

Stroke	Peak Current	10 to 90% Risetime (μs)	Continuing Current Duration (ms)
1	12.9	0.31	3.7
2	3.0	1.21	4.5
3	2.6	2.18	3.5
4	9.6	0.40	3.9
5	7.3	0.28	10.4
6	29.4	0.20	3.9
7	26.9	0.22	4.2
8	10.7	0.17	352.2
9	29.3	0.25	31.0
10	16.9	0.26	46.4
11	8.8	0.34	79.6

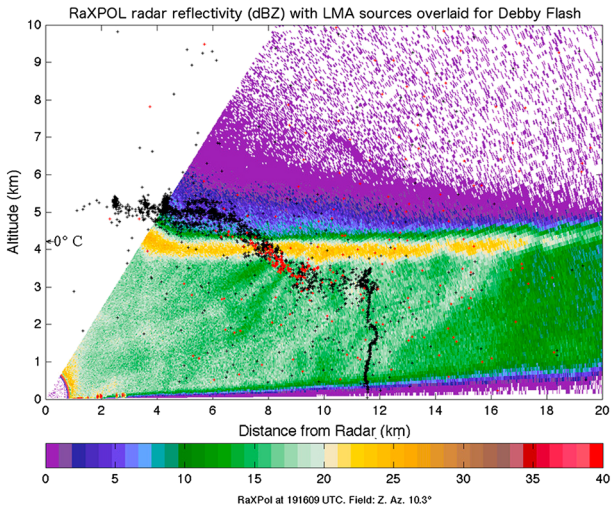

Figure 6. Range-height indicator (RHI) display of raw radar reflectivity, in dBZ according to the color scale, from the RaXPOL radar at 1916:09 UTC on 24 June 2012, about 4 s prior to the Debby flash. LMA sources within 10 km of the cross section are overlaid with points east (west) of the cross section shown in black (red). Due to a failing amplifier in the receiver chain, a loss of about 10 dB in signal strength and sensitivity occurred in the RaXPOL data during this event. The 0 °C designation is estimated from the location of the bright band.

and continuing current duration above about 2 A are given in Table 2. A flash composed of eleven strokes is on the high-end tail of the stroke-per-flash distribution for both natural and triggered lightning. A typical stroke number for natural negative cloud-to-ground lightning is 3–5, with 11 stroke flashes occurring about 1% of the time [*Rakov and Uman*, 2003].

3.1.2. The Initial Stage

[13] The initial stage (IS) of the flash, composed of the upward positive leader (UPL) and following initial continuous current (ICC), was relatively weak in current amplitude, duration, and charge transfer compared to those processes reported in the literature. The transition between the UPL and ICC is not well defined, as is the case for all triggered lightning flashes. The IS time duration is marked in the very low (VL) current record plotted in Figure 7. There is an absence of ICC pulses in the current record for the IS. The charge transfer mechanism for ICC pulses is thought to be similar to the *M* component mode of charge transfer [*Rakov and Uman*, 2003, pp. 176–182]. Most triggered lightning ISs contain at least one ICC pulse, which according to *Wang et al.* [1999], in Florida triggered lightning typically have a current amplitude between 100 A and 200 A and a 10 to 90% risetime between 200 and 800 μs. The average current, duration, and charge transfer of the IS of the Debby flash is 38.2 A, 202 ms, and 7.7 C, respectively. In contrast, the geometric mean of the same parameters is 96 A, 279 ms, and 27 C for 37 triggered flashes studied by *Wang et al.* [1999]; 99.6 A, 305 ms, and 30.4 C for 45 triggered flashes studied by *Miki et al.* [2005]; and 157.4 A, 547 ms, and

Table 3. The Geometric Means of the Initial Stage Duration, Charge Transfer, and Average Current Are Given for All Four Studies[a]

IS Study:	*Wang et al.* [1999]:	*Miki et al.* [2005]:	*Hill et al.* [2012]:	Debby Flash:
Sample size	26	45	9	1
Geometric mean of average current (A)	96	99.6	157	38.2
Duration (ms)	279	305	547	202
Charge transfer (C)	27	30.4	82.4	7.7
Max average current (A)	*	315.5	328	*
Min average current (A)	*	26.5	64	*
Max duration (ms)	*	782	945	*
Min duration (ms)	*	65	344	*
Max charge transfer (C)	*	135.6	225	*
Min charge transfer (C)	*	3	22	*

[a]For two studies where information was available, the maximum and minimum values for each parameter are listed. The initial stage current and charge transfer of the Debby flash were relatively small compared to those of other studies.

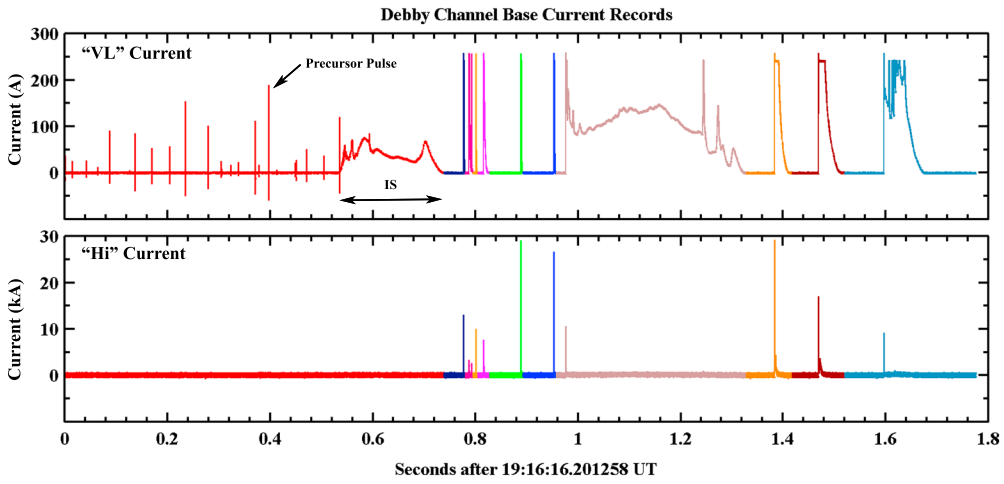

Figure 7. The channel base current measured at two different sensitivity levels for the initial stage and eleven return strokes, color coded as in Figure 5. The most sensitive measurement, VL, is plotted at the top with a saturation level of about 250 A, with the bottom plot "Hi" of least sensitivity on which no peak current saturates. On the VL current, precursor pulses, breakdown at the triggering wire tip, are evident. The time duration of the IS is marked.

Table 4. The Geometric Means of the Peak Current, Stroke Duration, Interstroke Interval, and No-Current Interval Are Given[a]

Parameter	*Fisher et al*. [1993]	Debby Flash
Peak current (kA)	15 (8)	11 (11)
Stroke duration (ms)	18 (30)	11 (11)
Interstroke interval (ms)	51 (22)	35 (11)
No-current interval (ms)	19 (22)	30 (10)

[a]The sample size (in parentheses) is given for each parameter of each study. Note the sample size was 10 instead of 11 for the no-current interval for the Debby flash because the third stroke took place while current was still flowing from the second stroke. The *Fisher et al*. [1993] data presented are from Kennedy Space Center.

82.4 C for 9 triggered flashes studied by *Hill et al*. [2012]. More detailed comparisons are given in Table 3. It should be noted that the studies by Wang et al., Miki et al., and Hill et al. all took place at the ICLRT, eliminating the impact of differing environmental characteristics on the parameters. The experimental setup described by *Hill et al*. [2012] is nearly identical to that of the present study. However, the lower current measurement limit of 20 A of Wang et al. and Miki et al. may have had some effect on their experimental results and statistical data, perhaps leading to an underestimate of the IS duration and charge transfer. Nevertheless, even without this bias, the average values for the IS reported by Wang et al. and Miki et al. exceed the Debby values. However, the Debby values are within the range of values reported by Miki et al.

3.1.3. Stroke Parameters and Exceptional Features

[14] The measured return stroke current waveform parameters under consideration are the following: peak current, stroke duration (time from start of return stroke until the current falls to zero as can be determined within the amplitude resolution of the measurement system, including continuing current), interstroke interval (time between successive return strokes), and no-current interval (the difference between the interstroke interval and the stroke duration). The parameters are measured as defined in section 3 of *Fisher et al*. [1993]. Statistical features of the parameters are summarized and compared to the previous literature in Table 3. Our values are similar to those Fisher et al. observed in rocket-triggered lightning at Kennedy Space Center, FL, given in Table 4. The sample size used in *Fisher et al*. [1993], 8 to 22 samples per parameter depending on the parameter, is larger than that of the present study and covers 8 flashes.

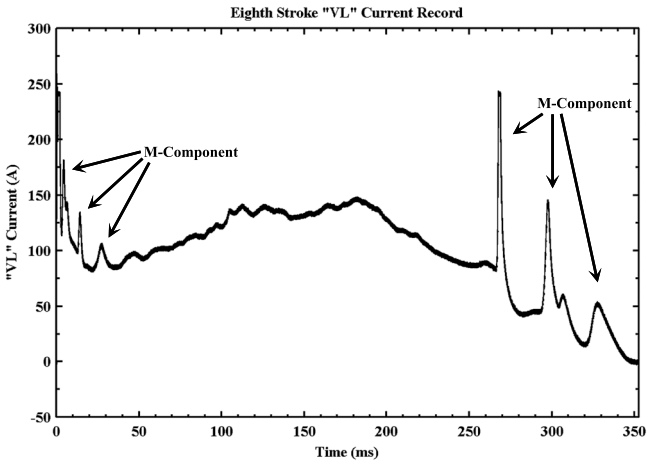

Figure 9. The VL channel base current waveform is shown for the continuing current following the eighth return stroke.

[15] Several aspects of the Debby flash were exceptional. Three return strokes had peak currents greater than 25 kA, one nearly 27 kA, and two exceeding 29 kA. These individual peak currents are nearly double the average peak current for triggered lightning strokes [*Fisher et al*., 1993] and subsequent strokes in natural lightning [*Berger et al*., 1975] to which triggered strokes are similar and approximately the average of natural negative first stroke peak currents [*Berger et al*., 1975]. The fact that three strokes exceeded 25 kA is in itself exceptional. Figure 8 shows the return stroke high "Hi" current records for each of the largest strokes (strokes 6, 7, and 9) of the flash. Although the current appears to reach zero within a 1–5 ms after the return stroke, the more sensitive current measurements show that significant current is flowing after that time. Figure 8a shows the current record from the sixth return stroke which had a peak current of 29.3 kA, the largest of the flash. A "very short" continuing current (defined as lasting 1 to 10 ms [*Shindo and Uman*, 1989]) of about 3.9 ms followed the sixth return stroke with at least one readily identifiable *M* component superimposed in the current. Figures 8b and 8c show the current record from the seventh and ninth return stroke, respectively. The seventh return stroke was also followed by a very short continuing current of about 4.2 ms with at least one *M* component superimposed in the current. The

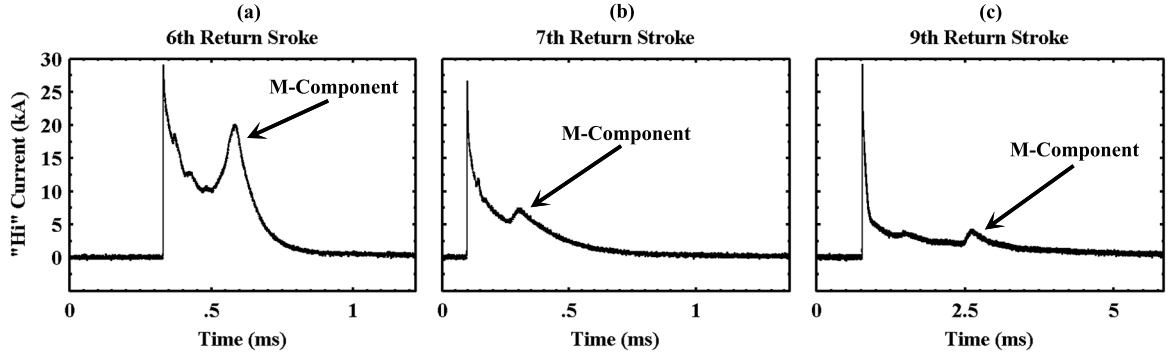

Figure 8. Channel base current waveforms for each of the three return strokes with peak currents greater than 25 kA.

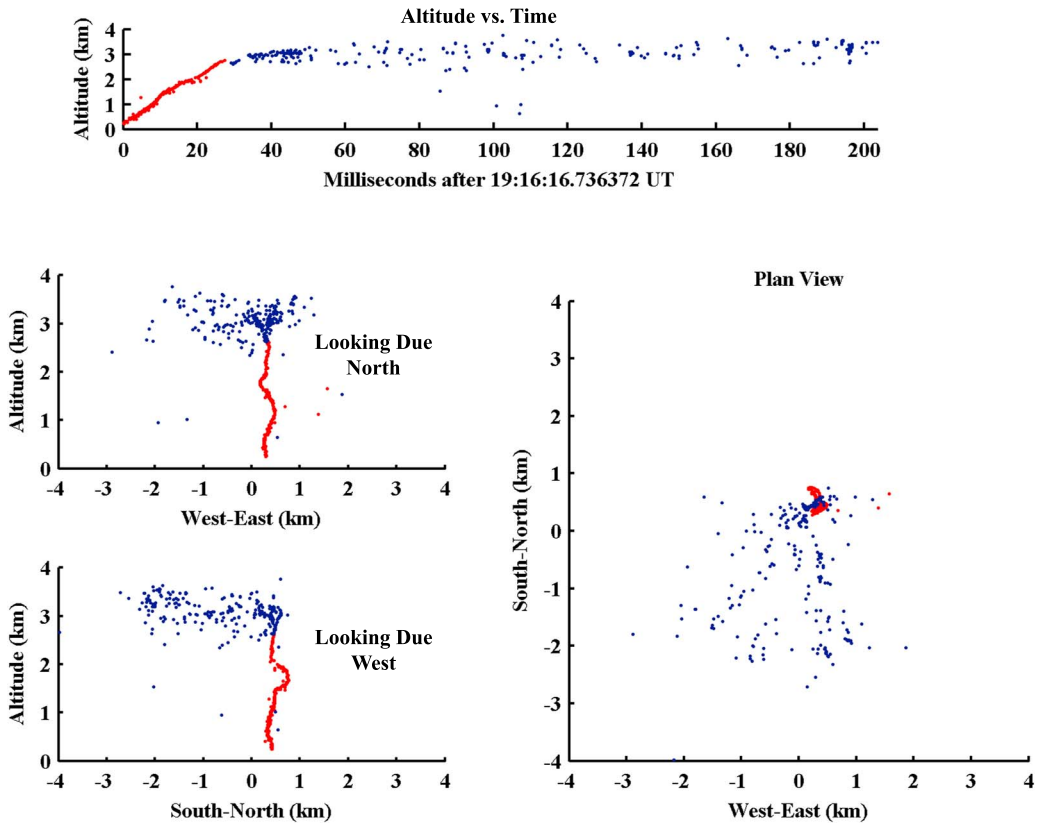

Figure 10. Four projections of the LMA data for the initial stage of the Debby flash. The red sources correspond to the unbranched portion of the UPL and the blue sources correspond to subsequent branching during the remainder of the initial stage, most clearly seen in the plan view.

ninth return stroke was followed by a "short" continuing current (defined as lasting 10 to 40 ms [*Shindo and Uman*, 1989]) of about 31 ms with at least one *M* component superimposed in the current. The very short and "short" continuing currents following the relatively high peak current strokes are features consistent with the findings of *Saba et al.* [2006]. *Saba et al.* [2006] further "found that negative strokes with peak current higher than 20 kA are never followed by continuing current durations greater than 40 ms", an observation with which our data are also consistent (see Table 2). *Berger et al.* [1975] measured current using an instrumented tower struck by natural, negative cloud-to-ground lightning. According to that study, 50% of first stroke peak currents exceeded 30 kA and only 5% of subsequent strokes, to which triggered lightning strokes are similar, exceeded 30 kA. The interstroke intervals preceding the return strokes of

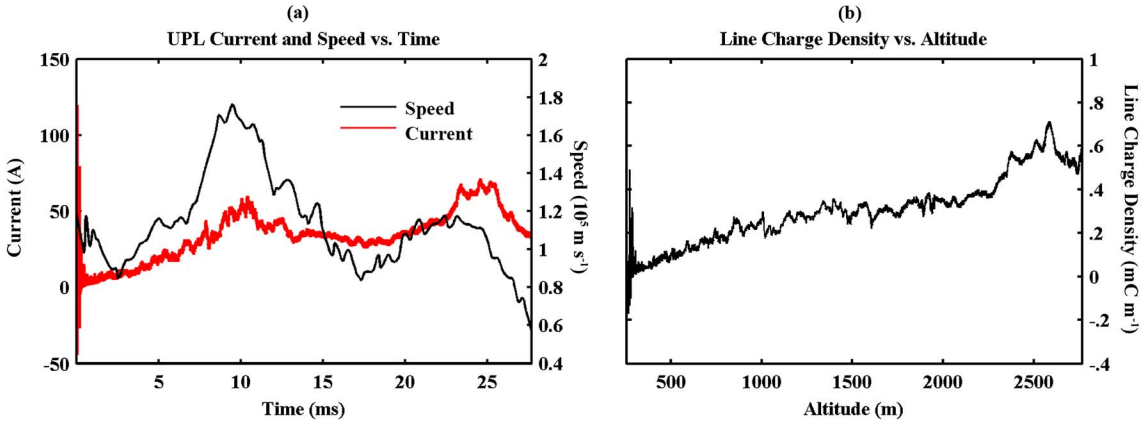

Figure 11. Plotted at left is the measured channel base current, colored red, and the measured speed of the UPL, colored black, versus time. At the right is the calculated line charge density variation versus altitude. Note that the altitude plot starts at 250 m since the UPL initiated at approximately that height.

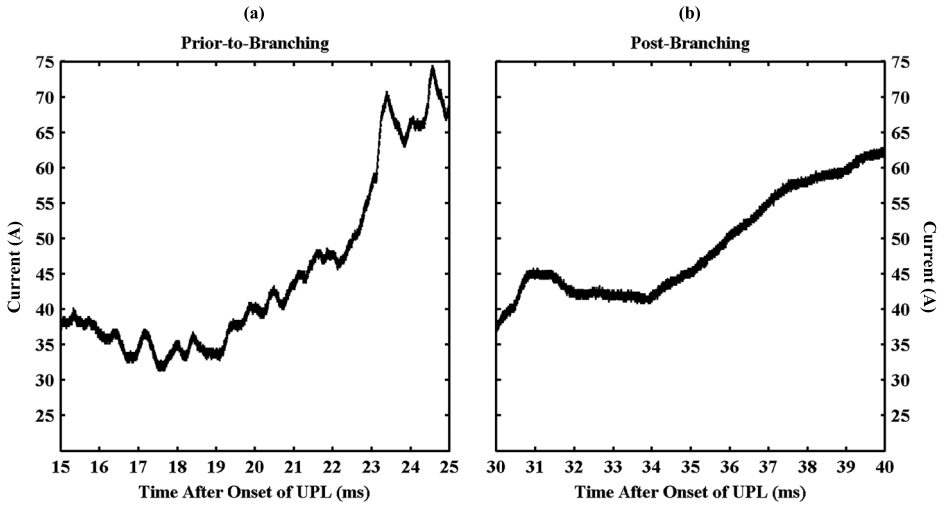

Figure 12. Ten milliseconds of the VL channel base current of the initial stage prior to the UPL branching at left and at right 10 ms of the same current record after the UPL branched. The current fluctuations seen in the left plot are absent in the plot on the right.

greatest peak current in the Debby flash were larger than the average for the flash, 35 ms, consistent with observations of *Schonland et al*. [1935] and *Jordan et al*. [1992] who found a positive correlation between the return stroke peak current and the previous interstroke interval. However, two strokes, the tenth and eleventh, exhibiting smaller peak currents, 16.9 kA and 8.8 kA, respectively, were also preceded by longer than average interstroke intervals and had larger than average stroke durations. Typically, the stroke duration (defined as the onset of return stroke through the end of any continuing current) and preceding interstroke interval are inversely related [*Shindo and Uman*, 1989]. Additionally, the unusually large stroke duration of the eighth stroke (including its continuing current) of approximately 352 ms, shown in Figure 9, transferred about 35 C of charge to ground. The average current for this portion of the flash was about 93.9 A. The continuing current following the eighth stroke will be further analyzed along with its associated LMA sources later (see Figure 18). Only 5% of strokes transferred charge greater than 15 C in the study of *Fisher et al*. [1993]. *Berger et al*. [1975] found that only 5% of first and subsequent strokes in natural lightning transferred charge in excess of 24 C and 11 C, respectively; and only 5% of flashes exceed charge transfers of 40 C when considering the sum of the charge transfer of each stroke and continuing current of a natural flash. A low-end estimate of the total charge transfer of the Debby flash is about 63 C.

3.2. LMA Observations and Supporting Measurements

3.2.1. The Initial Stage

[16] LMA data indicate that the initial stage (IS) consisted of an unbranched upward positive leader (UPL) that during its first 28 ms traveled at an average three-dimensional (3-D) speed of 1.1×10^5 m · s^{-1} over a 3.1 km path, including moderate-scale channel tortuosity, before branching at about 2.8 km in altitude. The method used here for calculating the 3-D speed of the UPL is similar to that of *Hill et al*. [2012] where sources were binned into intervals and then averaged spatially and temporally to produce new sources. Here, in addition, the new sources are processed by a filter to reduce the effect of outliers. Then a line is fit to the temporal variation of each spatial dimension using a shape preserving spline interpolant. The speed is calculated by numerically differentiating each fit line and vectorally summing the results together. The LMA sources emitted during the IS are plotted in Figure 10. Figure 10 has a similar format to Figure 5, except here, the LMA sources plotted are color coded based on the time before and the time after the onset of branching.

[17] The first VHF radiation source of the UPL was located at an altitude of about 250 m with an error of approximately 40 m. The LMA located a relatively large number of sources associated with the UPL owing to the relatively small baseline geometry of the LMA and the 10 μs time window length (reference *Hill et al*. [2012] for a comparison between 80 μs and 10 μs data).

[18] Figure 11a shows the UPL speed versus time and the channel base current versus time on the same plot for the unbranched portion of the UPL. According to equation (1), shown below, the charge per unit length, ρ_L, may be calculated by dividing current, I, by speed, v, a model that assumes that all new charge is deposited on newly formed sections of the channel including the corona envelope around the current-carrying channel [*Rakov and Uman*, 2003].

$$I = \rho_L \cdot v \tag{1}$$

[19] After approximately 5 ms, the speed of the UPL, v, appears to track the measured channel base current, I, indicating that the line charge density, ρ_L, of the channel is roughly constant. The line charge density, obtained in this manner, is plotted as a function of altitude in Figure 11b. The line charge density increases slowly with altitude from about 0.05 mC/m at a few hundred meters to about 0.55 mC/m near 3 km, an increase of a factor of 10. The change in line charge density with altitude is consistent with an increase in the electric field with altitude. The average line charge density of the unbranched UPL is 0.31 mC · m^{-1}.

[20] As noted above, when the UPL reached about 2.8 km in altitude, the UPL exhibited extensive branching, with

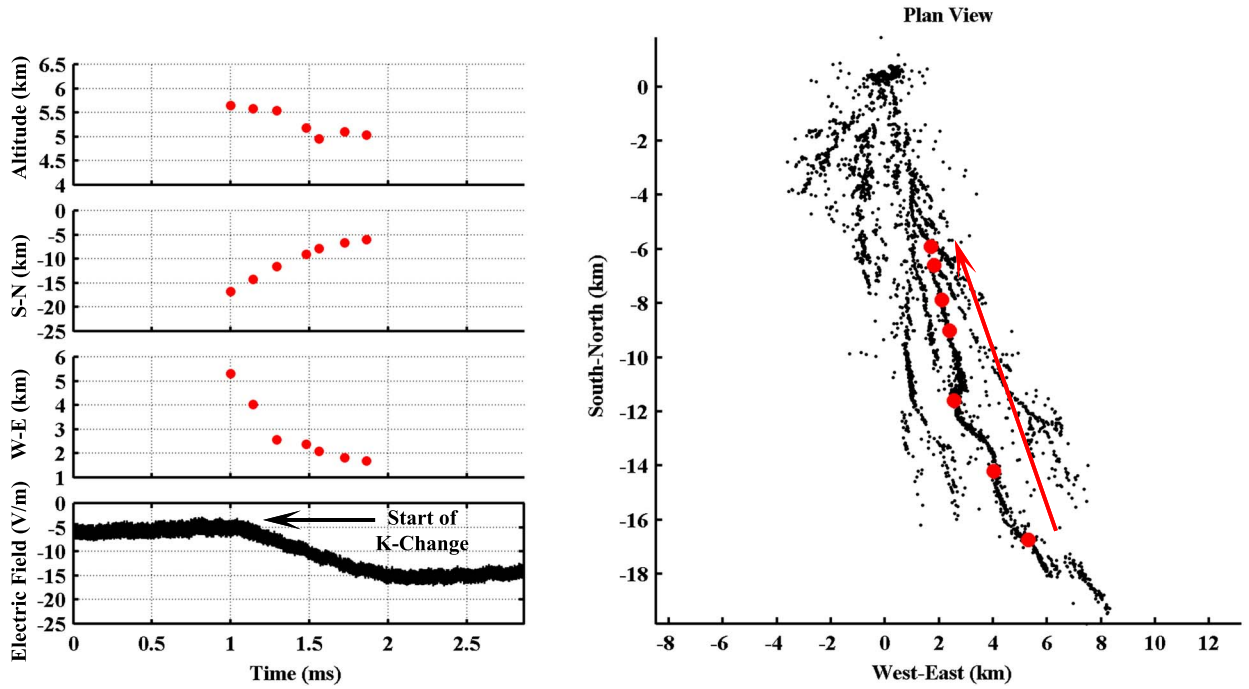

Figure 13. LMA sources correlated with a *K* change in the electric field record are shown at left and are colored red in the plan view given on the right. The sources colored black are from previous electrical breakdown. The red *K* change sources begin near the farthest extent of previous breakdown and travel back toward the base of the lightning channel.

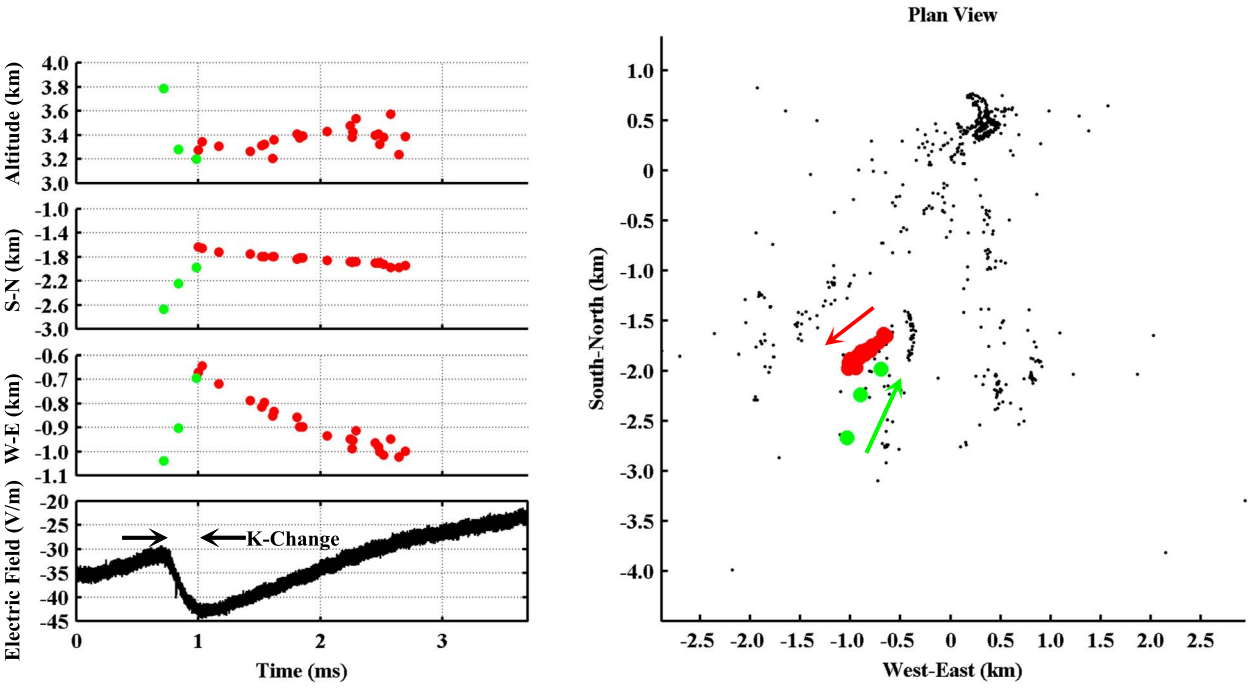

Figure 14. The LMA sources occurring during (green) and after (red) a *K* change in the electric field in the plots on the left. The plan view on the right shows the same *K* change-following sources colored red, with the sources corresponding to the preceding *K* change colored green. Again, the green sources travel from near the farthest extent of previous breakdown toward the channel base. The red sources travel in the opposite direction, apparently in virgin air.

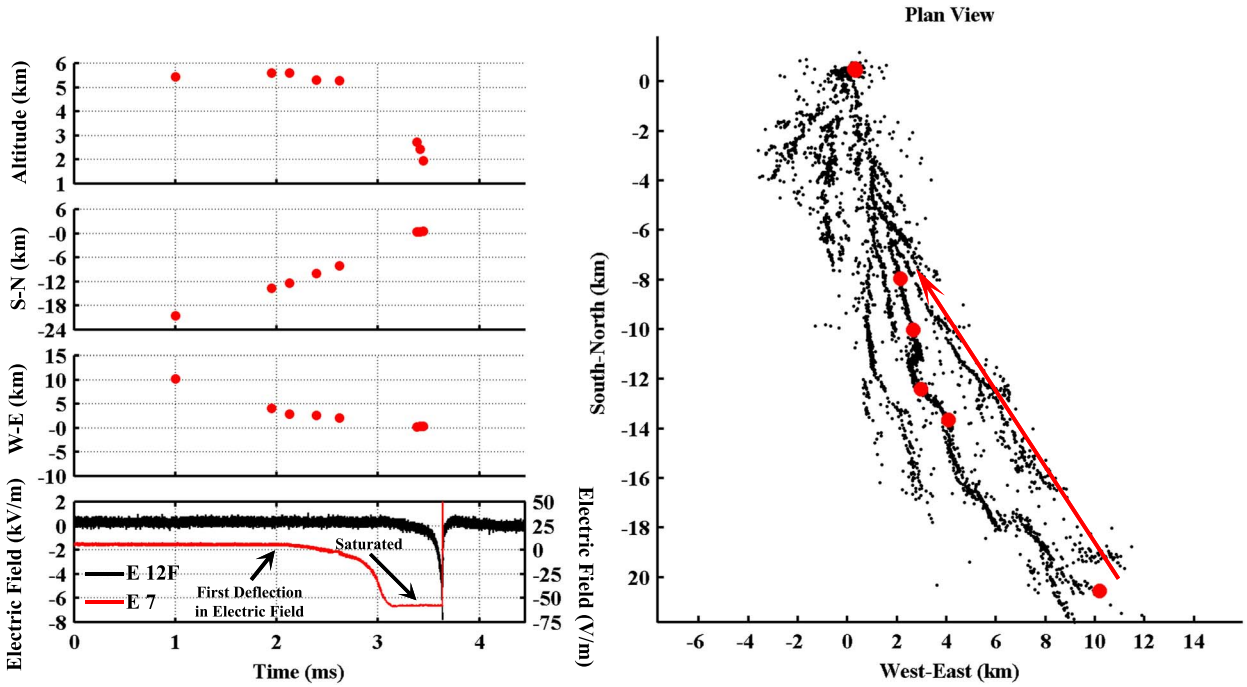

Figure 15. LMA sources and electric field associated with the dart leader preceding the tenth return stroke. The sources (colored red) begin near the farthest extent of previous breakdown (colored black), as seen in the plan view, and travel toward the channel base, with three sources located along the vertical portion of the channel to ground (top left plot of the altitude versus time). The right vertical scale on the lower left figure corresponds to the "E-7" curve and the left vertical scale corresponds to the "E-12 F" curve.

source locations becoming more diffuse. We subjectively infer that the UPL initially branched into two leaders, one of which had little subsequent activity, while the other served as the starting point for further branching and the remainder of the IS activity. At the time of the initial UPL bifurcation, around 33 ms after its onset, the current did not change significantly, only a slight increase in the current being detected. Between 28 and 33 ms, the current waveform appears to undergo a transition in its characteristic shape. Figure 12a shows a portion of the initial stage current before branching occurred and Figure 12b shows a portion of the initial stage current after branching, both portions being of the same duration. Prior to branching, the current waveform appears to be fairly jagged and erratic on a small (submillisecond) time scale, as seen in Figure 12a. After branching, the waveform still exhibits some small time scale fluctuations, but they appear to be smoothed out, as shown in Figure 12b. We postulate that the injection of current from multiple channels due to branching may cause an averaging effect on the total current measured at the channel base.

3.2.2. Subsequent Strokes

[21] After the IS and a 40 ms no-current period, there were eleven leader/return stroke sequences. The LMA sources, shown in Figure 5, constituting the VHF emission following the IS were divided into separate colors based on features of the channel base current. As previously noted, one color combines the no-current interval preceding a stroke, the stroke, and the continuing current following the stroke. LMA sources were surveyed and compared to correlated channel base current and electric field measurements. During the no-current interval preceding each stroke, particular attention was paid to sources associated with *K* changes leading up to the leader field change preceding the stroke. After the stroke and during following periods of continuing current, we focused on LMA sources correlated with *M* components. The following sections will discuss and give examples of the results of such analysis beginning with *K* changes and previously unnamed events following *K* changes, then dart leaders, and finally *M* components. A later section will qualitatively compare LMA sources during times of continuing currents with different "types" of continuing current waveforms as classified by *Fisher et al*. [1993].

[22] *Shao et al*. [1995] inferred from interferometer measurements that *K* events, dart leaders, and *M* components were essentially the same mechanism of charge movement. The three differed mainly in whether or not they eventually make an attachment to ground and the condition of the channel traversed in the cases in which a ground attachment is made. A *K* event, in their view, is an in-cloud dart leader which does not succeed in making a ground attachment. Typically, it is observed in electric field measurements as a "step" change in the electric field of the appropriate sign depending on the direction and polarity of charge motion in relation to the antenna. A dart leader succeeds in making a ground attachment, producing a return stroke which then neutralizes the charge deposited along the channel by the leader. Finally, an *M* component is viewed as an in-cloud dart leader that intercepts a channel already carrying a steady current, usually a continuing current following a return stroke. This mechanism is thought to produce the signature hump in the channel base current record, the current hump having generally a 100 μs to millisecond risetime. The high

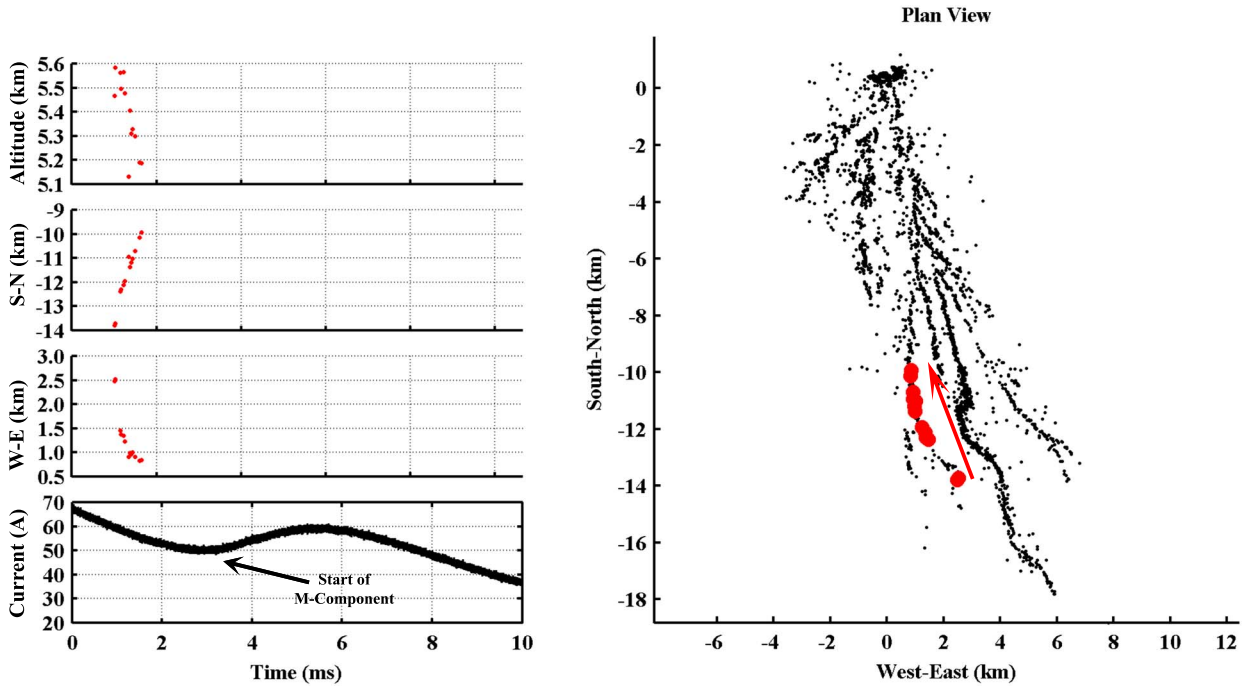

Figure 16. LMA sources which likely correspond to an *M* component observed in the current at ground. The sources (colored red) begin near the farthest extent of previous breakdown (colored black) and travel toward the channel base.

conductivity of the current-carrying channel apparently renders the path traversed to ground by the dart leader dispersive leading to the relative slowing in risetime of the current impulse associated with *M* components. In contrast, a dart leader incident on a channel with little or no current flowing propagates via a nonlinear breakdown process leading to a relatively fast return stroke current risetime.

[23] Dart leaders are generally not readily mapped by LMA systems. They travel paths of previous dielectric breakdown, whether in cloud or on the final length of channel to ground and hence produce less impulsive radiation than associated with electrical breakdown in virgin air (i.e., the leader tip of a propagating stepped leader). However, the conductivity of the channel traversed by some of the events studied were apparently sufficiently low over limited distances that breakdown was once again necessary for leader propagation. Thus, one would expect only a limited number of dart leader sources to be located by the LMA, as was generally the case.

[24] It should be noted that in the following plots of correlated LMA sources and electric field measurements shown in Figures 13, 14, and 15, no correction is made for the small (up to tens of microseconds) propagation delay between the time of LMA source emission and the corresponding measured electric field.

3.2.3. *K* Events

[25] *K* events are identifiable in the electric field record as a characteristic "step" change in the electric field called *K* changes. To correlate LMA sources with *K* events, the LMA sources must occur in close time proximity with the corresponding *K* change. From descriptions in previous interferometer studies of *K* events [*Shao et al*., 1995], the LMA sources travel from near the farthest extent of the previous breakdown back toward the channel base along a path previously mapped by LMA sources, that is, along a path of previous breakdown. The speed of propagation of the sources, as given in *Shao et al*. [1995], was roughly 10^6 to $10^7\,\mathrm{m\,s^{-1}}$. *Winn et al*. [2011] used an LMA and both ground-based and airborne electric field measurement to study *K* events associated with an intracloud flash and found similar results as *Shao et al*. [1995].

[26] An example of a *K* event is shown in Figure 13. It occurs prior to the ninth return stroke and moves negative charge toward the ICLRT electric field antenna. The sources, colored red, occur during a *K* change in the electric field and progress from near the farthest extent of previous breakdown illuminated by LMA sources back toward the base of the channel. The average speed of the sources is $1.4 \times 10^7\,\mathrm{m\,s^{-1}}$.

[27] Two other *K* events recorded during the Debby flash, one discussed in the following section, were studied and had similar characteristics, namely, they traveled from near the farthest extent of previous breakdown toward the channel base and propagated at an appropriate speed. The first *K* event occurred in the no-current interval preceding the first return stroke and traveled at an average speed of $4.6 \times 10^6\,\mathrm{m\,s^{-1}}$ (see next section) and the second *K* event occurred in the no-current interval preceding the ninth return stroke and traveled at an average speed of about $5.4 \times 10^6\,\mathrm{m\,s^{-1}}$.

3.2.4. LMA Sources After *K* Events

[28] In this section, an example of a previously unnamed process associated with LMA sources occurring immediately following a *K* event is presented along with supporting electric field measurements. The LMA sources shown in Figure 14 that occur after a *K* event create a channel extension in the opposite direction to the *K* event propagation, with about an order of magnitude slower propagation speed. The sources are fairly numerous over a relatively short extent. The direction of the electric field change indicates the motion of negative charge away from the antenna, whereas the

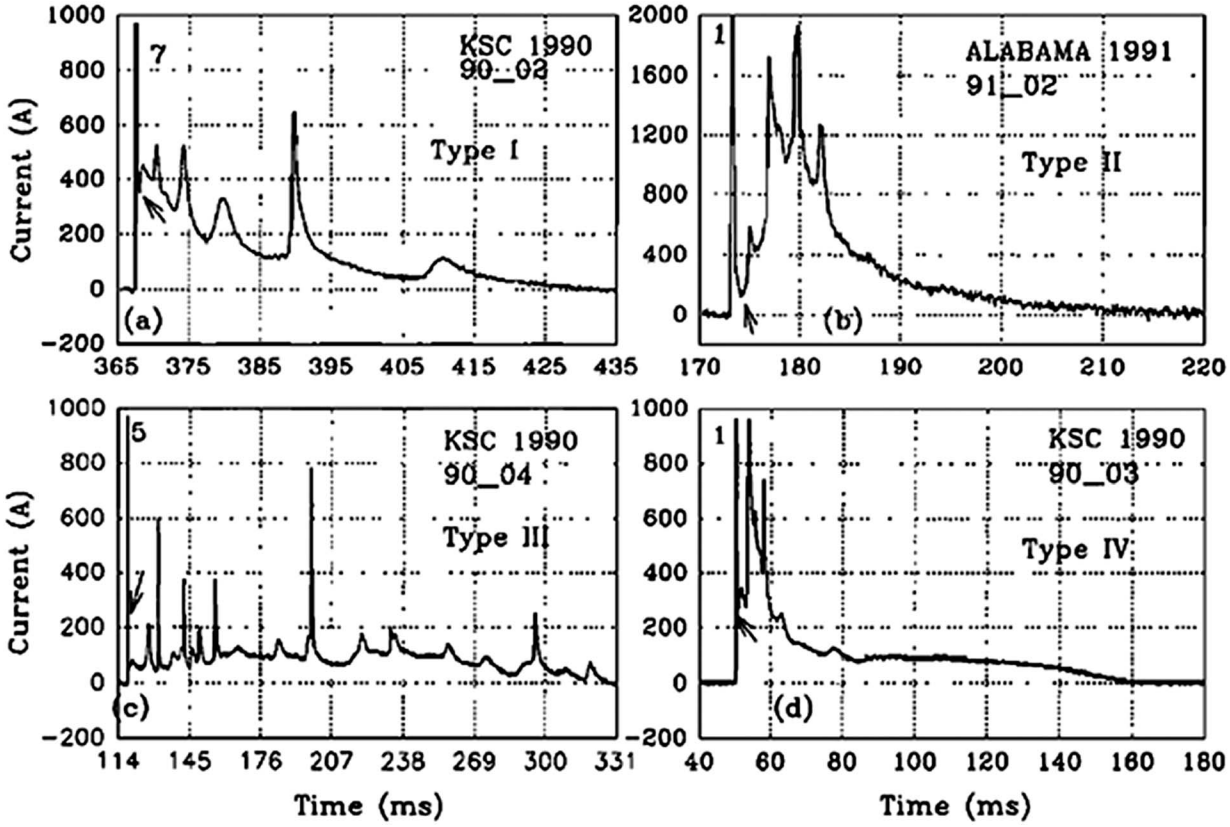

Figure 17. Typical examples of continuing current wave shapes from four different categories according to *Fisher et al*. [1993]. The arrows indicate the assumed beginnings of the continuing current. The numbers indicate the order of the return stroke in the flash. (a) Type I, more or less exponential decay with superimposed *M* current pulses; (b) Type II, a hump with superimposed *M* current pulses followed by a relatively smooth decay; (c) Type III, a slow increase and decrease of current with superimposed *M* current pulses throughout and relatively long duration; (d) Type IV, a hump with superimposed *M* current pulses followed by a steady plateau without pronounced pulse activity. Note the different time scales on the different continuing current wave shapes. Adapted from *Fisher et al*. [1993].

preceding *K* event produces electric field changes representative of negative charge motion toward the antenna. In Figure 14, the sources associated with the preceding *K* event are colored green and the subsequent breakdown is colored red. The LMA located 23 "red" sources during the no-current interval preceding the first stroke. The red sources begin just after the *K* change in the electric field record and the green LMA sources are associated with the corresponding *K* event. The average speed of the red sources was about 3.9×10^5 m s^{-1}, about an order of magnitude slower than the *K* event that preceded it. The slower propagation speed of the red sources would appear to indicate that the sources following the *K* event are traveling into virgin air, which would account for the reduced velocity of propagation from that of the *K* events. The red sources propagated over a relatively short distance (e.g., 600 m). Apparently, the negative charge deposited at the end of the *K* event channel was sufficient to launch a short-lived negative stepped leader.

3.2.5. Dart Leaders

[29] LMA sources associated with dart leaders are expected to have similar characteristics to those discussed for *K* events. Additionally, the time delay between the onset of the sources and onset of the return stroke observed at the channel base current should be consistent with the leader propagating at an expected speed over the LMA-measured path length to ground.

[30] The LMA located several sources associated with the dart leader preceding the tenth stroke, both in cloud and along the vertical channel to ground. The sources, colored red, are shown with supporting measurements in Figure 15. The in-cloud LMA sources began near the farthest extent of previous breakdown associated with the ninth stroke and traversed a path similar to the *K* event discussed above preceding the ninth stroke. The first source associated with the leader preceded the first observed electric field change by about 1.0 m s. The next source was located about 70 μs prior to the electric field change denoted on the E-7 curve of Figure 15 as the first deflection in the electric field. The absence of electric field variation with the first two dart leader sources may be due to the motion of a sufficiently small amount of negative charge associated with the leader, a lack of sensitivity of the electric field measurement, or a combination of the two. After the five in-cloud sources, no sources were located for 0.56 ms until three sources were located along the dart leader's generally vertical channel to ground.

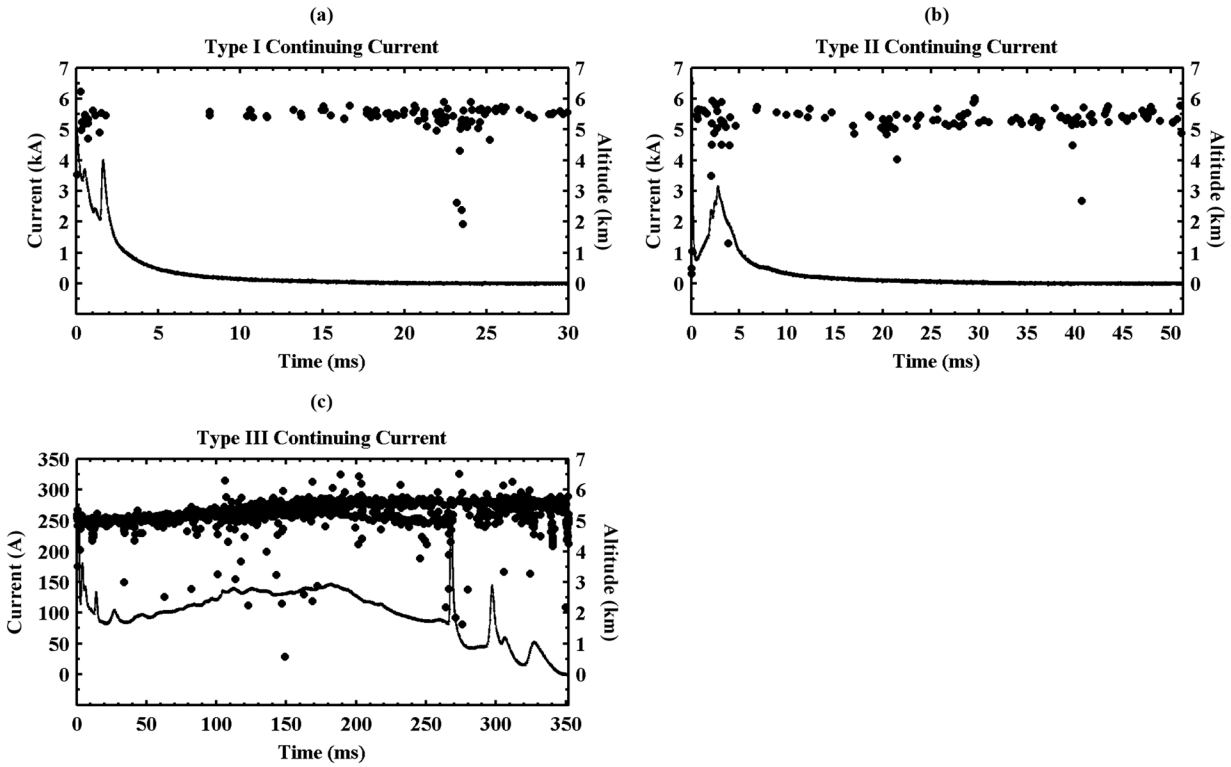

Figure 18. Three Debby continuing current waveforms characterized as in Figure 17. The LMA sources associated with the continuing current are overlaid with the channel base current. The "Type I" example is from the ninth stroke. The "Type II" example is from the tenth stroke. The "Type III" example is from the eighth stroke.

The in-cloud sources traveled at an average speed of about $9.6 \times 10^6\,\mathrm{m\,s^{-1}}$and the sources along the vertical channel traveled at an average speed of about $1.2 \times 10^7\,\mathrm{m\,s^{-1}}$. Given the time delay between the last in-cloud source and the first source along the vertical channel, the leader would have had to propagate at an average speed of $1.6 \times 10^7\,\mathrm{m\,s^{-1}}$, a likely underestimate of the actual speed considering channel tortuosity was not taken into account. The time delay between the last source located along the vertical channel and the onset of the return stroke was 0.2 ms, implying an average speed of about $9.7 \times 10^6\,\mathrm{m\,s^{-1}}$ for the remainder of the leader's propagation to ground.

3.2.6. *M* Components

[31] As noted above, *M* components are thought to begin in a similar fashion as *K* events and dart leaders, as sources traversing a path of previous breakdown, initiating near the farthest extent of previous breakdown and propagating at a speed of $10^6\,\mathrm{m\,s^{-1}}$ to $10^7\,\mathrm{m\,s^{-1}}$ toward the channel base. At some point, they encounter a channel carrying continuing current. Again, relatively few sources are expected to be located in association with the *M* component. In our study, identification of the sources associated with *M* components was made difficult by not having supporting electric field measurements. The electric field measurements were either saturated or responding to the field from the current flowing in the channel in relatively close proximity to the antenna. Because of this situation, the onset of the LMA sources cannot first be compared to a field change, as was the case with *K* events and dart leaders. The in-cloud sources associated with the *M* component are first identified as exhibiting properties previously mentioned with knowledge of the measured current flowing in the channel to ground. Then the time delay between the onset of the sources thought to be associated with an *M* component and the onset of the corresponding feature in the current record are taken into account. The average speed the *M* component would have had to travel in order to produce the observed current pulse is calculated by dividing the distance it would have to travel by the time delay.

[32] An example of LMA sources potentially correlated with an *M* component that occurred during the continuing current following the eighth stroke are shown in Figure 16. The sources (colored red) traveled at an average speed of about $7.1 \times 10^6\,\mathrm{m\,s^{-1}}$. The time delay between the last located source and the onset of the *M* component was 1.2 ms, indicating that the leader would have had to propagate at an average speed of about $1.1 \times 10^7\,\mathrm{m\,s^{-1}}$ over a 13 km path to ground, an underestimate considering channel tortuosity was neglected, to be consistent with the observation of an *M* component measured at the channel base.

3.2.7. Continuing Current

[33] In rocket-triggered lightning studies, *Fisher et al.* [1993] classified continuing current waveforms with durations greater than 10 ms into four different types. They note that not all continuing current waveforms are easily categorized into one of the four types. The four types of continuing current classifications are shown and given a brief explanation by *Fisher et al.* [1993, Figure 17]. A more recent paper by *Campos et al.* [2007] claimed two additional categories of continuing current waveforms. Using high-speed video observations, *Campos et al.* [2007] analyzed luminosity

versus time plots to study continuing current and *M* components in natural negative cloud-to-ground lightning. Since the additional continuing current classifications suggested by Campos et al. are not represented in our data set, they are not considered here. However, three of Fisher et al.'s continuing current types (all greater than 10 ms) are represented in the Debby flash current waveforms.

[34] Three of the last four strokes, strokes 8, 9, and 10, in the Debby flash were followed by continuing currents whose waveforms can be classified according to the descriptions in Figure 17. The continuing currents following the eighth, ninth, and tenth return strokes are shown in Figure 18 with their respective LMA sources overlaid using the altitude versus time projection. The waveforms are plotted on the appropriate amplitude scale to clearly show the waveform characteristics under consideration. Although it appears the current goes to zero midway through some plots, a more sensitive current measurement (not displayed in Figure 18) shows that current is still flowing at the 10–100 A level.

[35] The ninth return stroke is followed by a "Type I" continuing current, shown in Figure 18a, characterized as an essentially exponentially decaying current with *M* components superimposed on the current. Several LMA sources are located at the extent of previous dielectric breakdown as the current initially decays exponentially with three *M* components superimposed on the continuing current. After the last *M* component, there is a period of 6.3 ms where no LMA sources are located. Following this period, the LMA resumes locating sources while the current continues an exponential-like decay to zero at the channel base.

[36] The continuing current following the tenth return stroke is a good example of a "Type II" waveform, shown in Figure 18b, exhibiting a hump with *M* components superimposed on the current followed by a more or less exponential decay. Again, there are several LMA sources located as the current increases after the initial decay following the return stroke. There appear to be three *M* components superimposed in the current increase. A shorter period, 2.1 ms, ensues after this for which the LMA does not locate sources. The LMA then continues to locate sources while the current exhibits an exponential-like decay to zero, similar to the behavior of ninth return stroke.

[37] The continuing current following the eighth return stroke was briefly discussed in section 3.1 regarding stroke parameters and exceptional features because of its atypically long duration and large transfer (352 ms and 35 C). The continuing current following the eighth return stroke and the corresponding LMA sources are plotted in Figure 18c. The continuing current waveform can be classified into Fisher et al.'s "Type III" category because of its slow increase and then decrease in current with *M* components superimposed on the current. Unlike the previous two examples, LMA sources are more or less continually located for the duration of the continuing current. Several new channels are formed and constitute the majority of horizontal propagation of the discharge. The discharge travels over 10 km during the continuing current as shown in Figure 5e, indicating that the long continuing current following the eighth return stroke is associated with positive channel extension. It is interesting to note that the average current (93.9 A) and duration (352 ms) of the continuing current following the eighth return stroke are similar to the average current and duration of the initial stage of typical triggered lightning, as evident from Table 3.

[38] In all three cases presented, the flash was extended, differing mostly in degree, ranging from 1 km to 10 km. LMA sources located during the Type I and Type II continuing currents were similarly intermittent in character, whereas the LMA located sources during the Type III continuing current were more or less continuous. In both the Type I and Type II cases, a period of LMA inactivity followed the portion of the continuing current with *M* components. When the LMA begins locating sources once again, the current continues to decay to zero, seemingly unaffected by the new activity. The above also holds for the continuing current following the eighth return stroke, although there is not the same period of LMA inactivity described above, LMA sources are located after the last *M* component with no apparent influence on the current. Possibly, the LMA activity is indicating a channel extending which was not responsible for the continuing current and is therefore not observed in the current record.

[39] The duration of each of the three types of continuing current discussed above is similar to the respective continuing currents shown in Figure 17. In both studies, the Type III continuing current was of the longest duration, hundreds of milliseconds, and the Type I and Type II continuing currents lasted several tens of milliseconds.

4. Summary and Discussion

[40] LMA data with supporting measurements were presented for an eleven-stroke rocket-triggered lightning flash which took place in the absence of natural lightning during tropical storm Debby on 24 June 2012. Despite the absence of natural lightning activity and the relatively low cloud structure, the rocket-triggered Debby flash exhibited essentially the same phenomena, leader/return stroke sequences, continuing currents, *K* events, and *M* components, typically observed in both natural cloud-to-ground and normal triggered flashes. Additionally, the Debby flash exhibited several unusual features including three relatively high-peak-current return strokes and numerous and substantial continuing currents.

[41] The low altitude to which the initial stage (IS) of the Debby flash propagated calls into question the common view that the IS consists of an upward positive leader (UPL) that reaches the primary negative cloud charge region and is then followed by an initial continuous current (ICC). If the UPL of the Debby flash reached the primary negative charge region of the cloud, that charge was located two to three kilometers in altitude, a much lower altitude for primary negative charge than suggested in previous literature, 6 to 8 km, for deep convective clouds [e.g., *Rakov and Uman*, 2003]. *Hill et al.* [2012] also found that the UPL in the decaying portion Florida summer storms first propagated more or less vertically and then, upon reaching just above the 0 °C level, around 4.5 km above sea level (asl) altitude, propagated horizontally. In the Debby case, the zero degree level was also at 4.5 km asl. The vertical extent of the IS of the Debby flash reached no higher than about 3.5 km. The IS channel base current of the Debby flash was observed to undergo a transition in characteristic waveshape, which LMA data showed to be coincident with the first signs of the UPL branching, as shown in Figures 10 and 12. The branching may indicate a

point of transition between the leader and what might be termed the ICC portion of the IS. Perhaps, the branching exhibited by the UPL was a result of UPL contact with a region of diffuse negative charge. A charge region fairly low to the ground may be akin to a screening charge layer as opposed to one that results from the interaction of ice, supercooled water, and graupel typically thought to be typically involved in thunderstorm cloud electrification. Alternatively, the IS may be better described as consisting solely of a positive leader. The measured channel base current before and after the UPL branched was similar except for the decrease in high-frequency, low-amplitude perturbations during branching (Figure 12). Since there is no apparent characteristic other than branching that would indicate a transition from a UPL to an ICC, it is reasonable to suggest that the IS of the Debby flash, and perhaps of all triggered lightning flashes, consisted of only a branched positive leader.

[42] The first four strokes of the Debby flash appear to have initiated between 2.8 km and 4.4 km in altitude. *Waldteufel et al*. [1980] analyzed a triggered lightning flash in which 10 strokes were observed, using optical and electric field measurements, to originate in "clear air" at fairly low altitudes. The majority of the 10 strokes originated between 0.5 km and 2 km above ground level. The altitudes were determined by adjusting the altitude of a monopole charge model to fit observed electric field changes. The fitted values were compared against photographic (video) measurements and found to be consistent. All 10 strokes occurred within about 100 ms of the onset of the upward positive leader. The launching site was about 8.5 km displaced from the edge of a convective storm allowing for an unobscured view of the flash. Waldteufel et al. concluded that "negative charge, neutralized by each stroke, preexisted at the location corresponding to the extremity of each return stroke channel". They suggest that the charge may have originated either in the form of space charge or an "air parcel containing charged aerosols or droplets carried away" from the distant storm clouds. Although, the Debby flash was triggered in different conditions, and the strokes did not originate in clear air, it seems reasonable that the conclusion drawn from Waldteufel et al. may be relevant to the Debby flash. The low altitude of the first few strokes may be attributed to similar pockets of charge. Low-altitude charge regions would locally enhance the electric field at and above ground and give a much higher probability of successfully triggering a flash.

[43] If the IS of the Debby flash had been of average duration, around 300 ms as reported in previous studies, the first five return strokes would have been contained in the IS. Had that been the case, it is possible that, instead of the return strokes, ICC pulses would have occurred as the UPL contacted the regions that produced the return strokes since it is thought, as discussed in section 3, that the condition of the channel traversed to ground by a dart leader determines whether a return stroke or an *M* component is ultimately observed.

[44] *Mazur and Ruhnke* [1993] suggested that negative leaders (sometimes referred to as negative recoil leaders or negative recoil streamers) originate at the negative end of a positive leader channel which has become "cutoff" from the main lightning channel. (For a conceptual sketch of this scenario, refer to *Mazur and Ruhnke* [1993, Figure 14a].) In this scenario, negative charge would accumulate at the cutoff end of the leader channel as the positive leader end continues to propagate in the ambient electric field. As the negative charge accumulates, the potential difference between the cutoff location and the main lightning channel increases until the negative breakdown threshold is exceeded, at which time a negative leader is initiated and propagates toward the main channel. The negative leader would present itself as a *K* event, dart leader, or *M* component depending upon the condition of the channel it eventually traverses. The observations of *K* events, dart leader, and *M* component in section 3.2 are *inconsistent* with the negative leader initiation mechanism suggested by *Mazur and Ruhnke* [1993]. In all cases presented here, we found that the negative leaders are initiated near the farthest extent of previous positive leader channels. It is our view that negative leaders initiate when positive leader tips encounter discrete and localized pockets of negative charge near the farthest extent of the positive leader channels. Our observations are consistent with the interferometric observations of *Shao et al*. [1995].

[45] Finally, we wish to comment briefly on the triggered lightning hazard to launch vehicles and aircraft that the Debby weather situation represented. The material presented in this paper is clearly the best documented case of the triggering of lightning in a situation where natural lightning was not occurring. As such, it represents new data for devising launch rules for space vehicles. There have been two poorly documented but spectacular cases of launch vehicles triggering lightning in situations where there was no or little close natural lightning: Apollo 12 in 1969 and Atlas-Centaur 67 in 1987. Both events and the weather that produced them are reviewed in *Rakov and Uman* [2003], pp. 368-369, which gives references to the official reports for the two events. Apollo 12 represented the first time it was understood that launch vehicles could trigger lightning. Both events were associated with the passage of cold fronts through central Florida, in November for Apollo 12 and in March for Atlas-Centaur 67.

[46] **Acknowledgments.** This research was supported by DARPA NIMBUS grant HR0011-1-10-1-0061 and NASA NNK12EA79P. M. Biggerstaff was partially supported by National Science Foundation grant AGS-1063537. Further, we wish to thank N. Brooks and J. Jordan for their assistance in the rocket-and-wire triggered lightning experiment.

References

Berger, K., R. B. Anderson, and H. Kroninger (1975), Parameters of lightning flashes, *Electra*, *80*, 223–237.

Campos, L. Z. S., M. M. F. Saba, O. Pinto Jr., and M. G. Ballarotti (2007), Waveshapes of continuing currents and properties of M-components in natural negative cloud-to-ground lightning from high-speed video observations, *Atmos. Res.*, *84*, 302–310.

Fisher, R. J., G. H. Schnetzer, R. Thottappillil, V. A. Rakov, M. A. Uman, and J. D. Goldberg (1993), Parameters of triggered-lightning flashes in Florida and Alabama, *J. Geophys. Res.*, *98*(22), 887–902.

Hill, J. D., J. Pilkey, M. A. Uman, D. M. Jordan, W. Rison, and P. R. Krehbiel (2012), Geometrical and electrical characteristics of the initial stage in Florida triggered lightning, *Geophys. Res. Lett.*, *39*, L09807, doi:10.1029/2012GL051932.

Hill, J. D., J. Pilkey, M. A. Uman, D. M. Jordan, W. Rison, P. R. Krebhiel, M. I. Biggerstaff, P. Hyland, and R. Blakeslee (2013), Correlated lightning mapping array and radar observations of the initial stages of three sequentially triggered Florida lightning discharges, *J. Geophys. Res. Atmos.*, *118*, 8460–8481, doi:10.1002/jgrd.50660.

Jordan, D. M., V. P. Idone, V. A. Rakov, M. A. Uman, W. H. Beasley, and H. Jurenka (1992), Observed dart leader speed in natural and triggered lightning, *J. Geophys. Res.*, *97*, 9951–9957.

Krehbiel, P. R., R. J. Thomas, W. Rison, T. Hamlin, J. Harlin, and M. Davis (2000), Lightning mapping observations in central Oklahoma, *Eos. Trans. AGU*, *81*(3), 21–25, doi:10.1029/00EO00014.

Mazur, V., and L. H. Ruhnke (1993), Common physical processes in Natural and Artificially Triggered Lightning, *J. Geophys. Res.*, *98*(D7), pp. 12,913–12,930.

Miki, M., V. A. Rakov, T. Shindo, G. Diendorfer, M. Mair, F. Heidler, W. Zischanck, M. A. Uman, R. Thottappillil, and D. Wang (2005), Initial stage in lightning initiated from tall objects and in rocket-triggered lightning, *J. Geophys. Res.*, *110*, D02109, doi:10.1029/2003JD004474.

Peckham, D. W., M. A. Uman, and C. E. Wilcox Jr. (1984), Lightning phenomenology in the Tampa Bay area, *J. Geophys. Res.*, *89*, 11,789–11,805.

Rakov, V. A., and M. A. Uman (2003), *Lightning, Physics and Effects*, Cambridge Univ. Press, Cambridge, U.K.

Rison, W., R. J. Thomas, P. R. Krehbiel, T. Hamlin, and J. Harlin (1999), A GPS-based three-dimensional lightning mapping system: Initial observations in central New Mexico, *Geophys. Res. Lett.*, *101*(D21), 26,641–26,668, doi:10.1029/96JD01803.

Saba, M. M. F., O. Pinto Jr., and M. G. Ballarotti (2006), Relation between lightning return stroke peak current and following continuing current, *Geophys. Res. Lett.*, *33*, L23807, doi:10.1029/2006GL027455.

Schonland, B. F. J., D. J. Malan, and H. Collens (1935), Progressive lightning, part 2: The discharge mechanisms, *Proc. R. Soc. London Ser. A*, *152*, 595–625.

Shao, X. M., P. R. Krehbiel, R. J. Thomas, and W. Rison (1995), Radio interferometer observations of cloud-to-ground lightning phenomena in Florida, *J. Geophys. Res.*, *100*(D2), 2749–2783.

Shindo, T., and M. A. Uman (1989), Continuing current in negative cloud-to-ground lightning, *J. Geophys. Res.*, *94*(D4), 5189–5198.

Thomas, R. J., P. R. Krehbiel, W. Rison, S. J. Hunyady, W. P. Winn, T. Hamlin, and J. Harlin (2004), Accuracy of the lightning mapping array, *J. Geophys. Res.*, *109*, D14207, doi:10.1029/2004JD004549.

Waldteufel, P., P. Metzger, J. L. Boulay, P. Laroche, and P. Hubert (1980), Triggered lightning strokes originating in clear air, *J. Geophys. Res.*, *85*, 2861–2868.

Wang, D., V. Rakov, M. Uman, M. Fernandez, K. Rambo, G. Schnetzer, and R. Fisher (1999), Characterization of the initial stage of negative rocket-triggered lightning, *J. Geophys. Res.*, *104*(D4), 4213–4222, doi:10.1029/1998JD200087.

Winn, W. P., G. D. Aulich, S. J. Hunyady, K. B. Eack, H. E. Edens, P. R. Krehbiel, W. Rison, and R. G. Sonnenfeld (2011), Lightning leader stepping, K changes, and other observations near an intracloud flash, *J. Geophys. Res.*, *116*, D23115, doi:10.1029/2011JD015998.